Electronic Supplementary Information

Influence of vicinal surface on the anisotropic dielectric properties of highly epitaxial $Ba_{0.7}Sr_{0.3}TiO_3$ thin films

Guang Yao,[a] Yanda Ji,[a] Weizheng Liang,[a] Min Gao,[a] Shengliang Zheng,[b] You Wang,[b] Handong Li,[a] Zhiming Wang,[a] Chonglin Chen,[c] Yuan Lin*, [a]

[a] *State Key Laboratory of Electronic Thin films and Integrated Devices, University of Electronic Science and Technology of China, Chengdu, Sichuan 610054, P. R. China.*

[b] *Department of Materials Physics and Chemistry, Harbin Institute of Technology, Harbin 150001, P. R. China.*

[c] *Department of Physics and Astronomy, University of Texas at San Antonio, San Antonio, Texas 78249, USA*

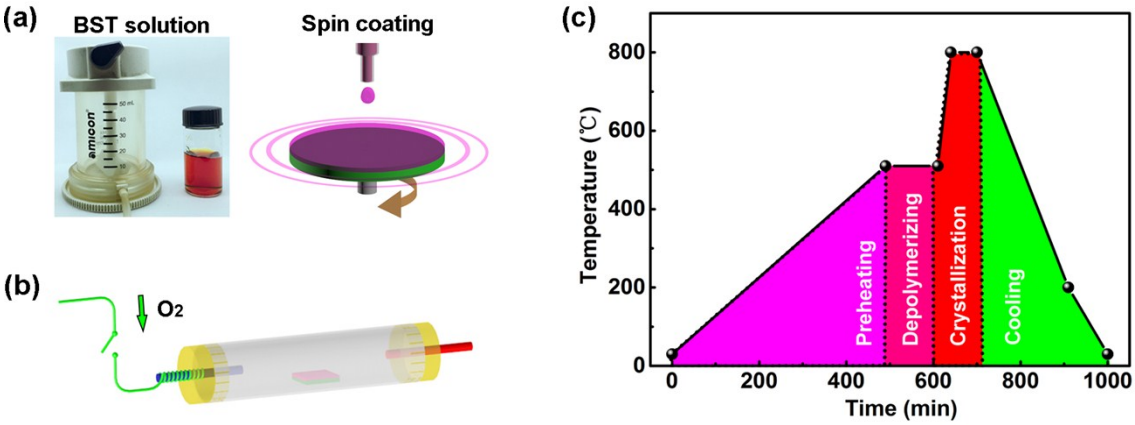

Fig. S1. The flow chart of the preparation process of epitaxial $Ba_{0.7}Sr_{0.3}TiO_3$ films using the PAD technique. (a) Solution preparation and spin coating. (b) Heat treatment in the tube furnace. (c) Temperature control of the heat treatment process.

The as-prepared BST precursor solution was spin-coated on the substrates with a spin rate of 3000 rpm for 30 s. The samples were then put into a tube furnace for heat treatment and the process can be described as the following. First, all the samples were heated to 510 °C slowly and maintained at that temperature for 120 minutes to depolymerize the polymer. Then the samples were annealed at 800 °C for 60 minutes for films crystallization. After that, all samples were cooled down naturally to room temperature. The whole heat treatment is in the flowing oxygen with a flow rate of 200 mL/min.

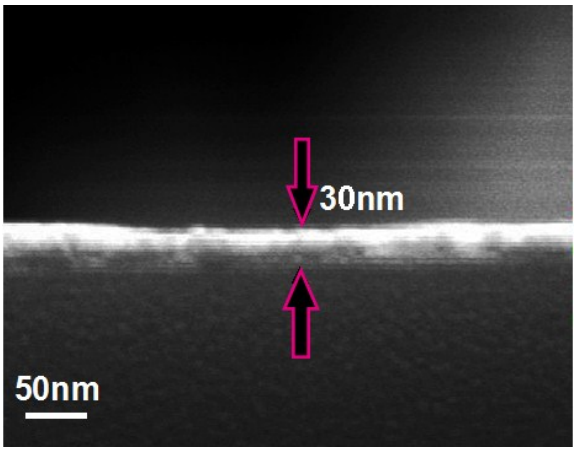

Fig. S2. A typical cross-section SEM image of the BST/LAO samples.

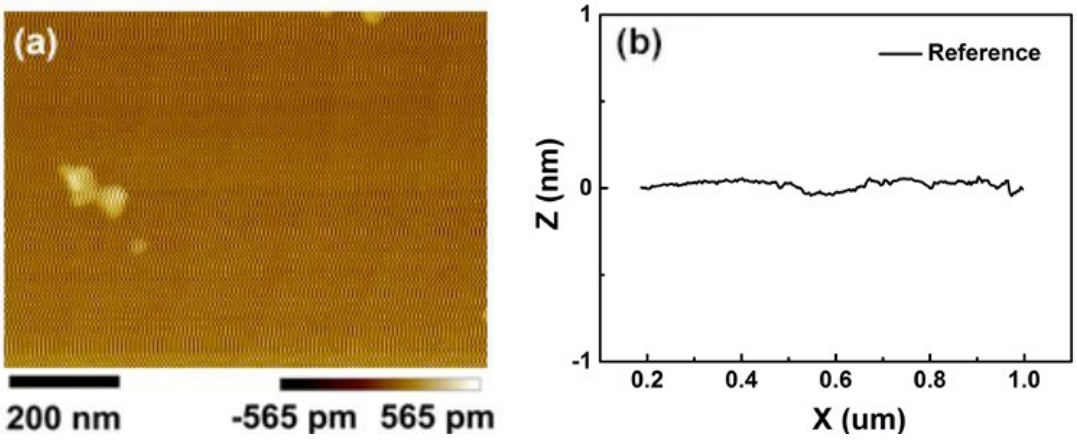

Fig. S3. The SPM image and a scanning line of the ordinary $LaAlO_3$ substrate.

As shown in the Fig. S3, the SPM image and a scanning line profile of the ordinary $LaAlO_3$ substrate was shown to indicate the flat surface compared with the vicinal substrates.

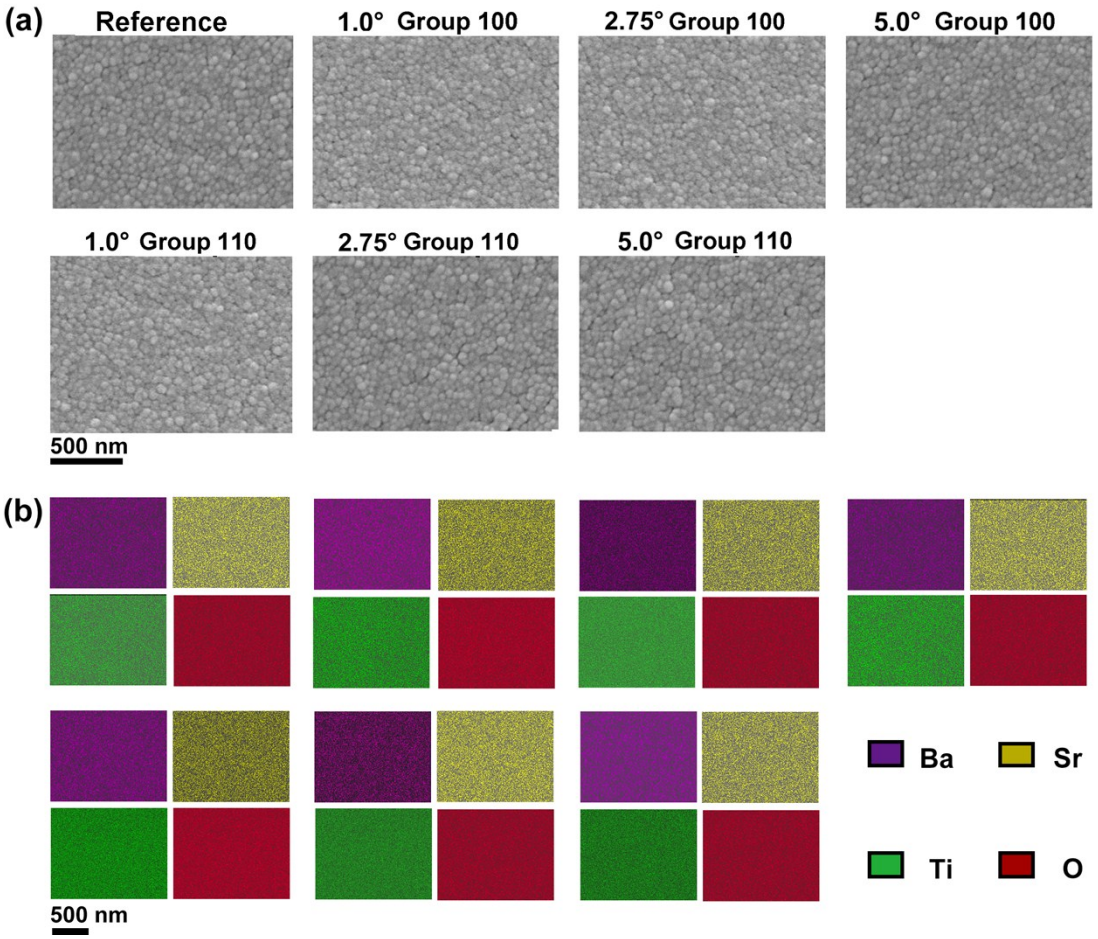

Fig. S4. Surface morphologies (a) and corresponding energy dispersive spectra (EDS) maps (b) of BST films grown on vicinal substrates with different miscut angles.

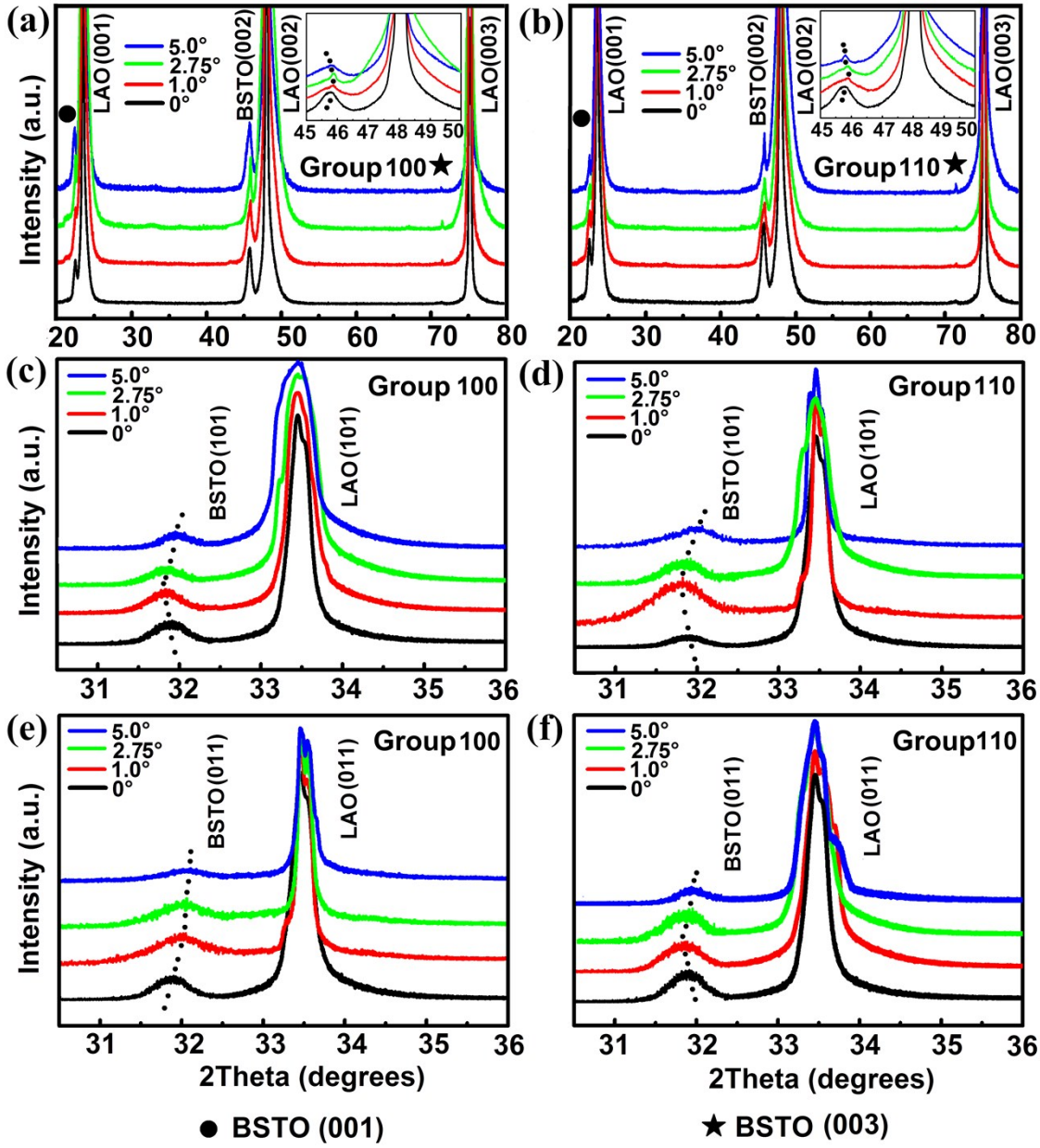

Fig. S5. XRD θ-2θ scanning patterns of the as-grown BST films on both groups of vicinal LAO substrates with different miscut angles. (a) and (b) are normal (χ = 0°) XRD θ-2θ scanning patterns for samples grown on group 100 and group 110 substrates, respectively. The insets are the fine XRD θ-2θ scanning patterns around the BST (002) peaks in a small range from 45° to 50°. (c) and (e) are tilted (χ = 45°) XRD θ-2θ scanning patterns from the diffractions of BST (101) and (011) for samples deposited on group 100 substrates, respectively. (d) and (f) are tilted (χ = 45°) XRD θ-

2θ scanning patterns from the diffractions of BST (101) and (011) for samples deposited on group 110 substrates, respectively.

Normal (χ = 0°) XRD θ–2θ scanning patterns for films grown on group 100 and group 110 substrates are shown in Figs. S5a and b, respectively. All the peaks in the patterns can be indexed by the (00*l*) diffractions from the perovskite structural BST and pseudocubic LAO, suggesting that the BST films were well fabricated with the preferred (001) orientation normal to the substrates. The diffraction patterns around the BST (002) peaks for all the samples were carefully rescanned and plotted in the insets of Figs. S5a and b. It is clearly shown that the peak position of BST (002) shifts with the miscut angle for samples in both groups. When the miscut angle increases from 0 to 1.0°, the BST peak shifts to a bigger angle, indicating a smaller lattice parameter along [001] direction. However, when the miscut angle further increases from 1.0° to 5.0°, the BST peak position moves back to an angle similar to that of the reference sample. It is worth noting that the change trends of peak shifting with the miscut angle are the same for samples in group 100 and group 110.

Tilted XRD θ-2θ scanning by setting χ = 45° were tested to get the strain information along both [100] and [010] directions. The incident X-ray was set to align the two in-plane orientations (φ= 0° and φ= 90°) in sequence. Figs. S5c and e are XRD scanning patterns from the diffractions of BST (101) and (011) for samples in group 100, respectively. Similarly, Figs. S5d and f are XRD scanning patterns from the diffractions of BST (101) and (011) for samples in group 110, respectively. Based on the results, in group 100, it is found that the change of BST (101) peak with the

miscut angle has an opposite changing trend compared with BST (002) and the BST (011) peak shifts very little. Meanwhile, for the films deposited on group 110 substrates, both changing trends of BST (101) and (011) peaks are opposite with that of BST (002). Thus, the lattice parameters for both in-plane and out-of-plane can be determined by carefully analyzing the normal and tilted scanning spectra, which were extracted based on Bragg spacing equation and discussed in the manuscript. Obviously, in both groups, the films deposited on the 1.0° miscut substrates have the largest peak shift in both out-of-plane and in-plane directions.

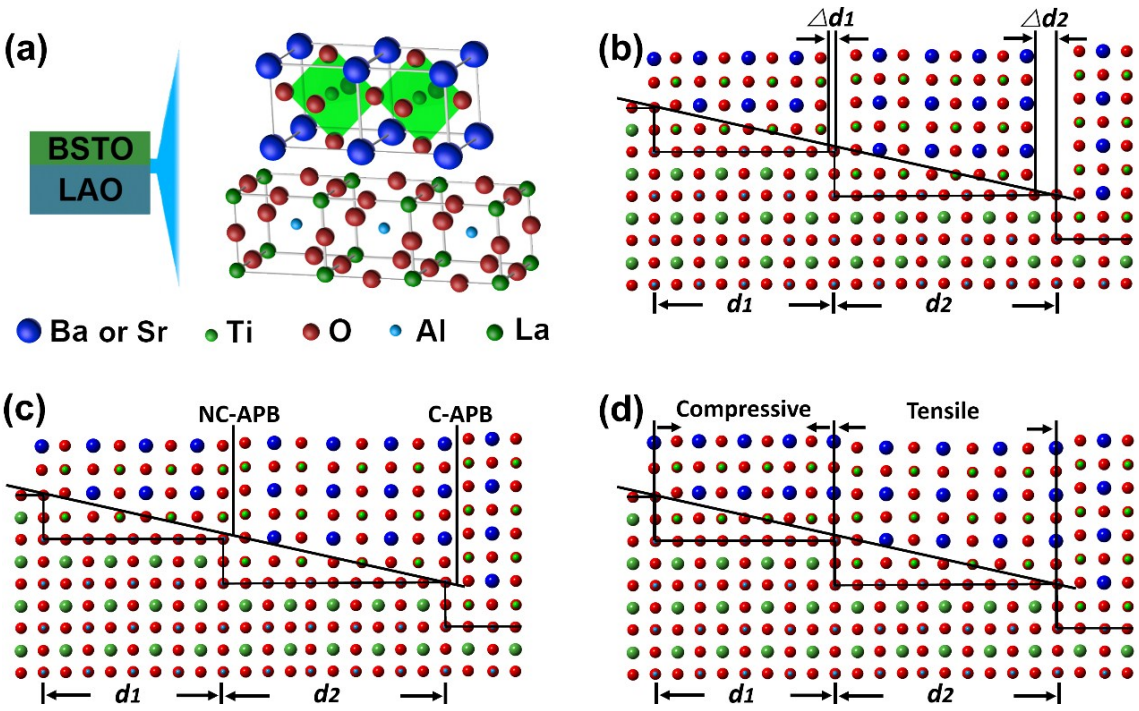

Fig. S6. Schematic diagram showing atomic arrangement of the BST film on surface step terrace of the vicinal (001) LAO substrate. (a) Crystal structures of LAO and BST. (b) The generation of the "residual mismatching gap" at the end of the step terrace. (c) The formation of conservative and nonconservative antiphase domain boundary. (d) The formation of locally strained domain with conservative antiphase domain boundary induced by the "residual mismatching gap".

To understand the lattice deformation mechanism of the as-grown samples, mismatching strains introduced by surface step terraces of the vicinal substrates should be taken into consideration. Literature report indicated that the surface of LAO (001) substrate is terminated with LaO while the BST film initiates with the TiO_2 plane when the film is deposited at the temperature range from 750 to 830 °C.[1] In addition, growth of the first TiO_2 monolayer on the terraces can also be assumed to be in the following sequence: the first row adjacent to the step would be the Ti-O atomic chain, hereafter it is the second row of the O-O chain, then third row of the Ti-O, the

fourth row of the O-O chain, and so on.[2] Thus, we simply use the type of termination in Fig. S6 to demonstrate the basic idea of the SST matching model. Crystal structures of LAO substrate and BST films were shown in Fig. S6a. According to "Surface-Step-Terrace" (SST) model, the surface-step-terrace dimension of a LAO substrate cannot exactly accommodate integer unit cells or atomic planes of the BST film. Theoretically, due to the difference in the lattice constant between the epitaxial film and substrate, the ''SST residual matching gap'' (Δd) will be generated at each edge of the LAO step terrace, as seen in the Fig. S6b. The terraces with different dimensions will result in the formation of different domains (antidomains) in the films. As shown in Fig. S6c, if the substrate surface terrace width is equal to n unit cells of the BST films, the initial row and the last row will be Ti-O atomic chains, and conservative antiphase domain boundary (C-APB) will form at the end of step terrace. Otherwise, when a terrace width is equal to (n + 1/2) BST unit cells, nonconservative antiphase domain boundary (NC-APB) will form at the end of step terrace. However, because of ionic bonding of the oxide films, unlike metal or semiconductor thin films, oxide thin film growth requires a good match in the combination of positive and negative charge balance. Therefore, it is highly impossible to form a nonconservative antiphase domain boundary at the end of the substrate terrace, since a large interface strain energy will be generated due to the same charge repulsion at the domain boundary and interface. Therefore, it is highly likely that the residual matching gap will be released via the formation of locally strained domains.[3-5] Practically, one more or less BST unit cell may deposit on the step terrace forming an in-plane compressive

or tensile strain region, as shown in Fig. S6d. Atoms of BST film rearrange on surface step terrace depending on terrace dimensions to occupy the entire width of each terrace length (*d*), introducing “SST strain” in the film.

Table S1. The corresponding calculated information for films grown on group 110 substrates.

Sample	T_w(nm)	T_w/a_s	n_s	a_s*n_s(nm)	$(a_s*n_s)/a_f$	n_f	a_f*n_f(nm)	Stress	Percentage
1.0° off(1-unit-cell-high)	30.94	81.01	81	30.93	77.12	77	30.88	Tensile	99%
			82	31.32	78.07	78	30.29	Tensile	1%
1.0° off(2-unit-cell-high)	61.87	162.02	162	61.87	154.25	154	61.77	Tensile	98%
			163	62.25	155.18	155	62.17	Tensile	2%
2.75° off (4 unit-cell-high)	44.97	117.75	117	44.68	111.40	111	44.52	Tensile	25%
			118	45.06	112.35	112	44.92	Tensile	75%
2.75° off(5 unit-cell-high)	56.21	147.19	147	56.14	139.96	140	56.15	Compressive	81%
			148	56.52	140.92	141	56.55	Compressive	19%
5.0°off	35.68	93.42	93	35.52	88.55	89	35.70	Compressive	58%
			94	35.90	89.51	90	36.10	Compressive	42%

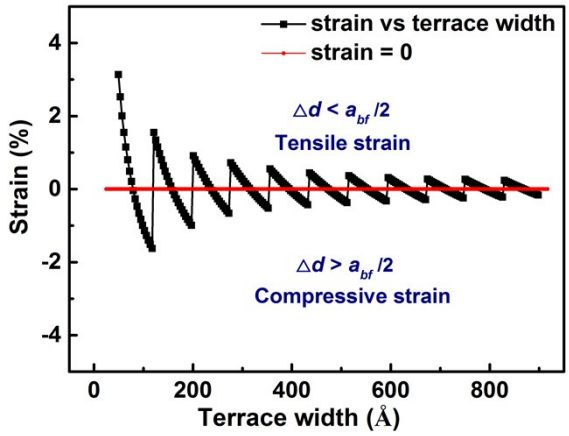

Fig. S7. Surface-step-terrace-induced strain $\delta = (a_f - a_{bf}) / a_{bf}$ of films grown on vicinal substrates with different terrace widths. The films bare tensile strain above the red line (strain=0)，and bare compressive strain below the red line.

The method to further evaluate the strain state on terrace steps has been reported earlier.[6] "SST residual matching gap" (Δd) will be generated at each edge of the $LaAlO_3$ step. One more or less BST unit cell may deposit on step terrace forming an in-plane tensile or compressive strain region to get a good match in the combination of positive and negative charge balance and fit the terrace width. The residual matching gap can be calculated using

$$\Delta \mathrm{d} = \mathrm{d} - N_f a_{bf} \quad (1)$$

where d is the terrace dimension on the substrate, a_{bf} is bulk lattice constant of the film material (3.98 Å for BST), and N_f is the maximum number of the unit cells in the film that one terrace can accommodate to ensure a positive Δd value.

If Δd is smaller than a_{bf} /2, one less BST unit cell may deposit on step terrace forming an in-plane tensile strain region, and the residual space will be averaged by all unit cells in the film on the terrace and the atomic spacing in the film will be elongated ($a_f > a_{bf}$).

$$a_f = a_{bf} + \frac{\Delta d}{N_f} \tag{2}$$

Otherwise, if Δd is larger than $a_{bf}/2$, one more BST unit cell may deposit on step terrace forming an in-plane compressive strain region. In other words, a new (Ba, Sr) O- plane must be inserted into the residual space and thus the atomic spacing in the film is compressed ($a_f < a_{bf}$).

$$a_f = a_{bf} + \frac{\Delta d - a_{bf}}{N_f + 1} \tag{3}$$

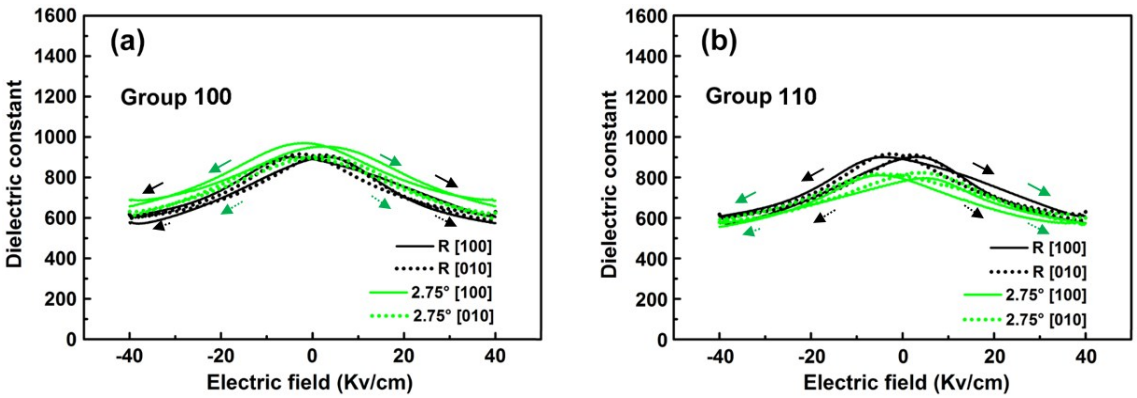

Fig. S8. In-plane ε-E curves of BST films at 100 kHz. (a) ε-E curves of BST films grown on the reference and 2.75° vicinal substrates in group 100. (b) ε-E curves of BST films grown on the reference and 2.75° vicinal substrates in group 110.

References

1. H.-J. Gao, C. L. Chen, B. Rafferty, S. J. Pennycook, G. P. Luo and C. W. Chu, *Appl. Phys. Lett.*, 1999, **75**, 2542-2544.
2. J. C. Jiang, Y. Lin, C. L. Chen, C. W. Chu and E. I. Meletis, *J. Appl. Phys.*, 2002, **91**, 3188-3192.
3. C. Ma, M. Liu, C. Chen, Y. Lin, Y. Li, J. Horwitz, J. Jiang, E. Meletis and Q. Zhang, *Sci. Rep.*, 2013, **3**, 3092.
4. C. Ma, M. Liu, G. Collins, H. Wang, S. Bao, X. Xu, E. Enriquez, C. Chen, Y. Lin and M.-H. Whangbo, *ACS Appl. Mater. Interfaces*, 2013, **5**, 451-455.
5. Q. Zou, M. Liu, G. Wang, H. Lu, T. Yang, H. Guo, C. Ma, X. Xu, M. Zhang and J. Jiang, *ACS Appl. Mater. Interfaces*, 2014, **6**, 6704-6708.
6. H. Lu, C. Zhang, H. Guo, H. Gao, M. Liu, J. Liu, G. Collins and C. Chen, *ACS Appl. Mater. Interfaces*, 2010, **2**, 2496-2499.